

An Euler Maruyama Scheme Exploration of the CEV Process

John Lee

December 15, 2023

Abstract

This paper provides a comprehensive exploration of the Constant Elasticity of Variance (CEV) process, a stochastic differential process integral to financial mathematics. It delves into the historical development of the process, highlighting its role in option pricing and its advancements over the traditional Black-Scholes model. Central to this study is the 'constant of elasticity' term, α , which characterizes the relationship between the underlying asset price and volatility within the CEV process, offering a more realistic depiction of market dynamics. The paper investigates the mathematical underpinnings of the CEV process, particularly focusing on the transition density function and its norm-decreasing property within the $\alpha < 1$ regime. Additionally, the research employs the Euler-Maruyama scheme to simulate the CEV process for various option strike prices ($K = 90, 100, 110$), comparing simulated call and put option prices to analytically computed values for different values of the elasticity parameter, alpha. Additionally, an analysis of discretization errors for negative values of the elasticity parameter is performed, due to high error measurements. This research provided me with valuable insights into the applicability, theoretical, and computational aspects of the CEV process.

1 Introduction

Options, as financial instruments, grant the holder the right, but not the obligation, to buy or sell an underlying asset at a predetermined price within a specified time frame. This definition encapsulates two primary types of options: calls, which provide the right to purchase, and puts, which offer the right to sell. In the realm of financial mathematics, options have become a fundamental instrument, providing investors with the flexibility to hedge risks or speculate on future market movements. The concept of options dates back to ancient times, but the modern framework for options pricing emerged in the 20th century, coinciding with the development of sophisticated financial markets. The Chicago Board Options Exchange (CBOE) was established in 1973, marking the first organized options exchange, which greatly increased the accessibility and standardization of options trading.

With the onset of mass options trading, research in options pricing schemes began skyrocketing. IN 1973, the landmark Black-Scholes model, publicly introduced by Fischer Black

and Myron Scholes, revolutionized the field by providing a systematic approach to pricing European-style options [1]. This model, which assumes constant volatility and a log-normal distribution of stock prices, has been celebrated for its simplicity and mathematical elegance, and it laid the foundation for the contemporary options market. Despite its groundbreaking impact, the Black-Scholes model has notable limitations, primarily the assumption of constant volatility. This limitation was made evident in the market crash of 1987 and has since been widely criticized, as empirical studies show that market volatility is stochastic and varies over time [6]. These limitations spurred further research into alternative models that could more accurately capture market behaviors.

One such development is the Constant Elasticity of Variance (CEV) process, introduced by John Cox in 1975. The CEV model addresses a critical limitation of the Black-Scholes model by allowing the volatility of the underlying asset to be a function of the asset price itself, thereby introducing a 'smile' effect in implied volatility that is observed in real markets [2]. The CEV model's flexibility in modeling volatility dynamics makes it a valuable tool for pricing options in markets exhibiting stochastic or patterned volatility, offering a more nuanced and realistic approach compared to the Black-Scholes model.

In this study, I explore several mathematical properties and provide simulations of the CEV process. The paper is organized as follows. First, in Section 2, I introduce the mathematics of the CEV process, discussing its relationship to the Black Scholes model and other mathematical properties. Then, in Section 3, methodology and simulations of the CEV process through the Euler-Maruyama discretization scheme are presented, with comparisons to analytical values. I take a closer look at the discretization scheme for negative values of α in Section 3.3, and lastly, some conclusions and future work are discussed in Section 4.

2 Mathematics of the CEV Process

2.1 Black Scholes Model

The Black-Scholes Model described in [1] is primarily recognized as a partial differential equation with an analytical form determining the price of a European call option at expiry. However, the Black-Scholes Model can also be understood as a stochastic process, the underlying stochastic differential equation a direct application of Geometric Brownian Motion,

$$dF = \mu dt + \sigma_{LN} F dW \quad F(0) = F_0 > 0 \quad (1)$$

where F is the price of an underlying asset, μ is a drift term, σ is the annual lognormal volatility of a stock, and dW is a Weiner process. The stochastic differential equation is defined up to a time T in years. The volatility term, σ_{LN} , remains constant throughout the entire period, confirming the constant volatility assumption.

2.2 SDE of the CEV Model

The CEV process is a time-diffusion process containing a conceptually simple extension of geometric Brownian motion,

$$df = \mu dt + \sigma F^\alpha dW, \quad F(0) = F_0 > 0 \quad (2)$$

where α is an additional parameter known as the constant of elasticity. In order to maintain the dimensionality of σ , we let

$$\sigma = \sigma_{LN} F^{1-\alpha} \quad (3)$$

be the instantaneous value of volatility.

Now, depending on the value for the constant of elasticity, α , three unique regimes can be identified within the CEV process as shown via the Fokker-Plank equations by Feller in [3]. These regimes can be interpreted from both a financial or mathematical perspective as follows

1. $\alpha > 1$. In this regime, σ is inversely related to price and leverage ratios increase, a commonly observed occurrence in equity markets. This relationship is rigorously explored in [9].
2. $0.5 < \alpha < 1$. In this regime, σ is positively related to price, a common occurrence in commodity markets [4]. Additionally, a boundary of $F = 0$ is attainable and absorbing. This absorption results in interesting mathematical behavior discussed in Section 2.4
3. $\alpha < 0.5$. This regime also results in a positive correlation between volatility and price. The boundary $F = 0$ is attainable and can be either reflecting or absorbing.
4. $\alpha = 1$. While not a regime, this case mathematically evaluates back to the original Black-Scholes diffusion process.

2.3 X-Transform

For the rest of this paper, we focus our exploration by eliminating the drift term, $\mu = 0$, and address only the mathematics of the $\alpha < 1$ case. We choose $F = 0$ to be an absorbing boundary condition for all α .

$$dF = \sigma F^\alpha dW \quad F(0) = F_0 > 0, \alpha < 1 \quad (4)$$

When observing the CEV process, as mentioned in [7], it is significantly advantageous to deal with the transformed variable, X , and its corresponding stochastic differential equation

$$X = \frac{F^{2(1-\alpha)}}{\sigma^2(1-\alpha)^2}, \quad dX = \delta dt + \sigma\sqrt{X}dW, \quad \delta = \frac{1-2\alpha}{1-\alpha} \quad (5)$$

The SDE in equation 5 is easily verified by Ito's lemma (see Appendix A) and is known as the squared Bessel process with δ degrees of freedom.

For positive integer δ , the Bessel process governs the squared distance, X , from the origin of a Brownian particle in δ spatial dimensions, and is known to have a non-central chi-squared distribution

$$\rho_{\chi^2}(x; \delta, \lambda) = \frac{1}{2} \left(\frac{x}{\lambda}\right)^{\nu/2} \exp\left[-\frac{x+\lambda}{2}\right] I_\nu(\sqrt{x\lambda}), \quad \nu = \frac{\delta}{2} - 1 \quad (6)$$

where $\chi^2(x; k, \lambda)$ is the non-central chi-squared distribution with k degrees of freedom and non-centrality parameter λ , and I_ν is the modified Bessel function of the first kind with index ν [7]. In the CEV process, δ may not necessarily be a positive integer (as it depends on α), but this relationship is important for the next section.

2.4 Transition Density Function

By solving the Fokker-Plank equations using Laplace Transforms on the squared Bessel process in equation 5, the transition density function

$$\rho_\delta(X_T, T; X_0) = \frac{1}{2T} \left(\frac{X_T}{X_0} \right)^{\nu/2} \exp \left[-\frac{X_T + X_0}{2T} \right] I_{-\nu} \left(\frac{\sqrt{X_T X_0}}{T} \right) \quad (7)$$

can be found. Refer to [5] for a detailed derivation. In [7], it is noted that an inspection of the TDF reveals a relation to the non-central chi-squared distribution as follows,

$$\rho_\delta(X, T; X_0) = \rho_{\chi^2} \left(\frac{X_0}{T}; 4 - \delta, \frac{X}{T} \right) \frac{1}{T}. \quad (8)$$

The $F = 0$ absorbing boundary mentioned in Section 2.2 is preserved as $X = 0$ in the transformation to X . Due to the absorbing nature of the $X = 0$ boundary, it is possible to lose probability mass. In [7], a direct integration of $\rho_\delta(X, T; X_0)$ is taken, finding

$$\int_0^\infty \rho_\delta(X, T; X_0) dX = \Gamma \left(-\nu; \frac{X_0}{2T} \right) \leq 1 \quad (9)$$

where Γ is the normalized incomplete gamma function

$$\Gamma(n; x) = \frac{1}{\Gamma(n)} \int_0^x t^{n-1} e^{-t} dt. \quad (10)$$

Cases of equation 9 with strictly less than one are known as norm-*decreasing*, while cases of equality to one are known as norm-*preserving*. In our simulations in Section 3, we can verify the absorption ratio using this relationship.

2.5 Analytical Options Pricing Formula

From the CEV process, an analytical options pricing formula can be established just like the Black-Scholes equation. For a European at-expiry option, its value can be determined by the equation

$$C = E[\max(F_T - K, 0) | F_0] = \int_K^\infty (F - K) \rho_\delta(F, T; F_0) dF, \quad (11)$$

where F_T is the final price of the underlying, K is the strike price, and T is the expiration date. According to [8], the integral in equation 11 can be computed in the $\alpha < 1$ regime as

$$C_{\alpha < 1} = F_0 \left[1 - \chi'^2 \left(\frac{\tilde{K}}{T}; 4 - \delta, \frac{X_0}{T} \right) \right] - K \chi'^2 \left(\frac{X_0}{T}; 2 - \delta, \frac{\tilde{K}}{T} \right), \quad \tilde{K} = \frac{K^{2(1-\alpha)}}{\sigma^2(1-\alpha)^2} \quad (12)$$

providing an analytical solution for European call options. Additionally, we can find the equivalent put option prices through put-call parity:

$$P_{\alpha < 1} = C_{\alpha < 1} - F_0 + K. \quad (13)$$

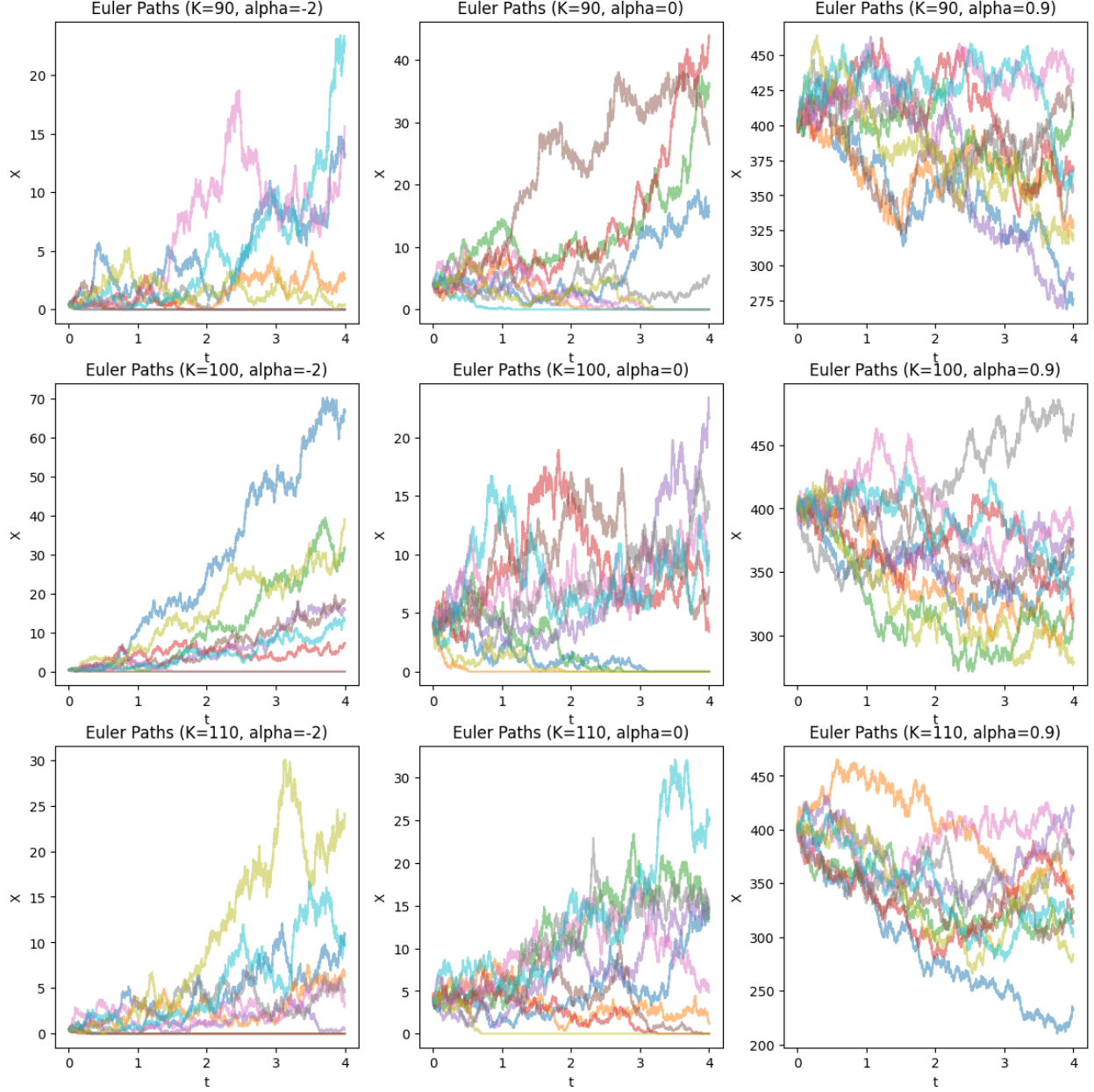


Figure 1: Euler path simulations of X for $K = 90, 100, 110$ and $\alpha = -2, 0, 0.9$

3 Simulations of the CEV Process

3.1 Methodology

To simulate the CEV process, we employ an Euler-Maruyama scheme over equation 5. I let the discretization be $dt = 0.001$ and the number of samples be $N = 10^6$. I also let $F_0 = 100$, $T = 4$ years, and presumed an annual lognormal volatility of $\sigma_{LN} = 0.5$. Strike prices of $K = 90, 100, 110$ and alpha values $\alpha = -2, -1, 0, 0.1, \dots, 0.9$ were explored. On a 12th Gen Intel(R) Core(TM) i5-12600K, 3.69 GHz, with 10-core multiprocessing, simulating

one set of parameters took roughly 6 minutes.

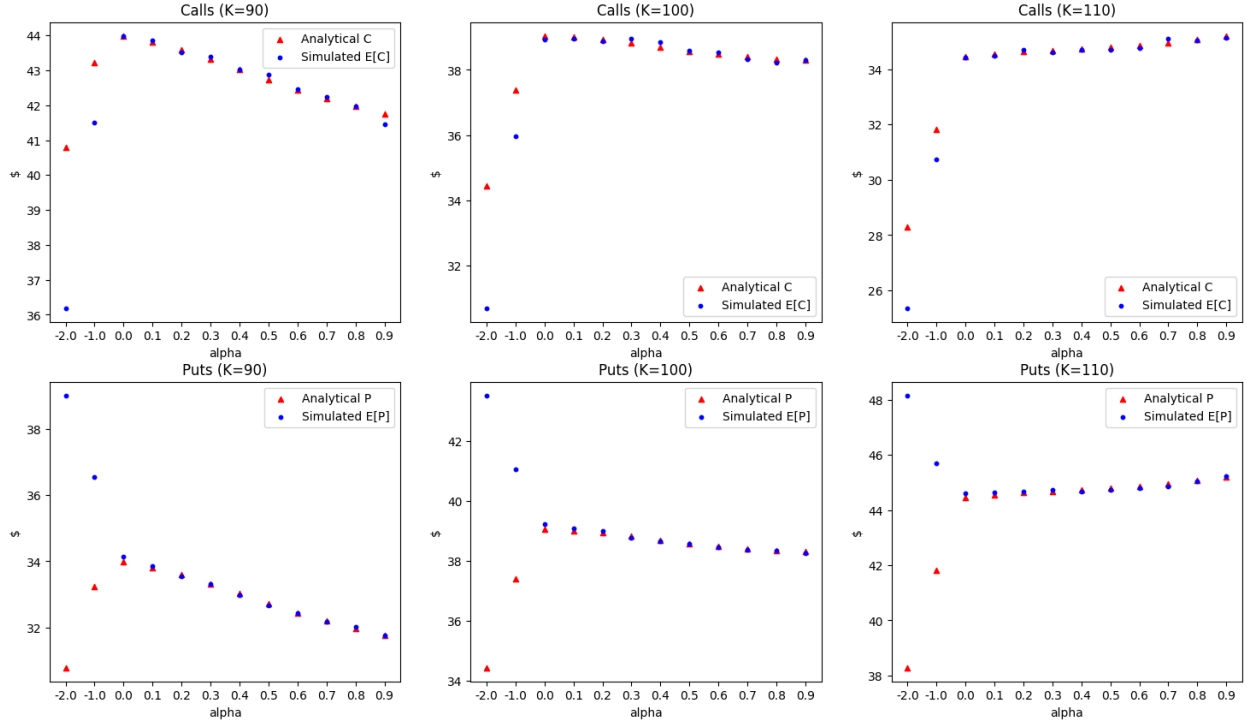


Figure 2: Comparison of Euler simulated prices to analytical options prices. Large deviations in $\alpha < 0$ are analyzed in Section 3.3

3.2 Simulations

Path simulations can be found in Figure 1. Final computed simulation prices are found in Figure 2. Computed prices are from the formula found in Section 2.5. To find exact values and standard error measurements, tabular forms of the data can be found in Appendix B. Additionally, in Section 2.4, we established that the absorption rate for simulated paths could be computed by a gamma function relationship. We verify our simulations with a plot of alpha versus absorption ratio in Figure 3.

3.3 Discretization Error in $\alpha < 0k$

In both Figures 2 and 3, it is clear that the Euler scheme is somehow failing for the $\alpha < 0$ case. However, when observing the paths in Figure 1, it is not evident where precisely the Euler simulation is going wrong. I conducted a simple discretization test to observe the rate of convergence and error measurements, changing $dt = 0.002, 0.001, 0.0005$. Results are shown in Figure 4. The reduction in error seems to appear linearly related to the \log_2 of dt . Extrapolating this linear relationship, it appears that dt must be shrunk roughly 9 and 45 times from $dt = 0.0005$ for accurate simulations of $\alpha = -1$ and $\alpha = -2$, respectively. However, this would be computationally intractable and consume significant amounts of memory.

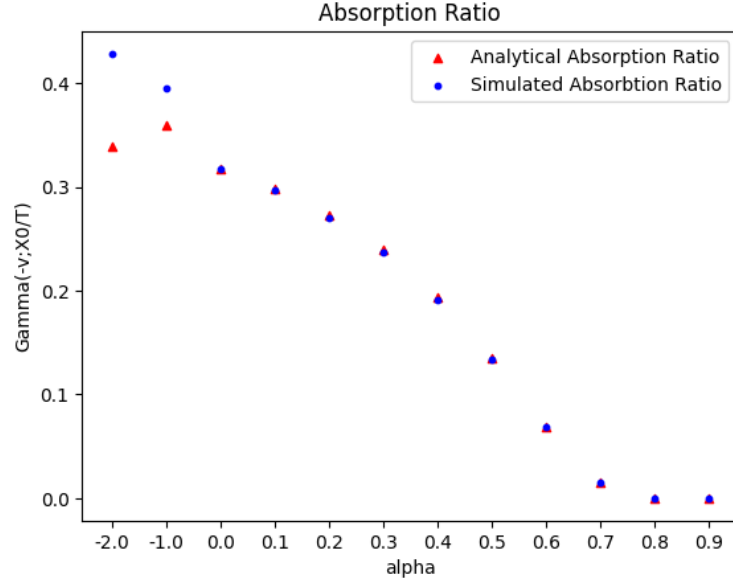
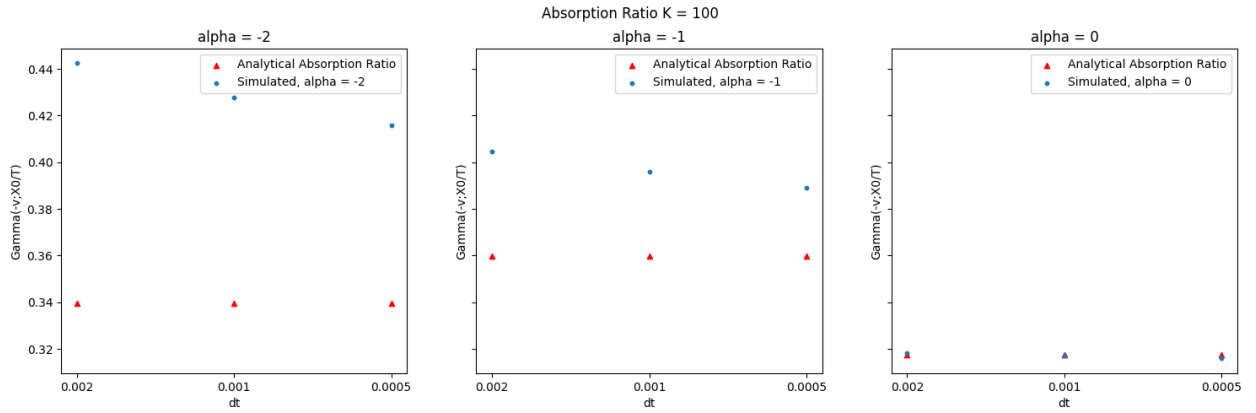
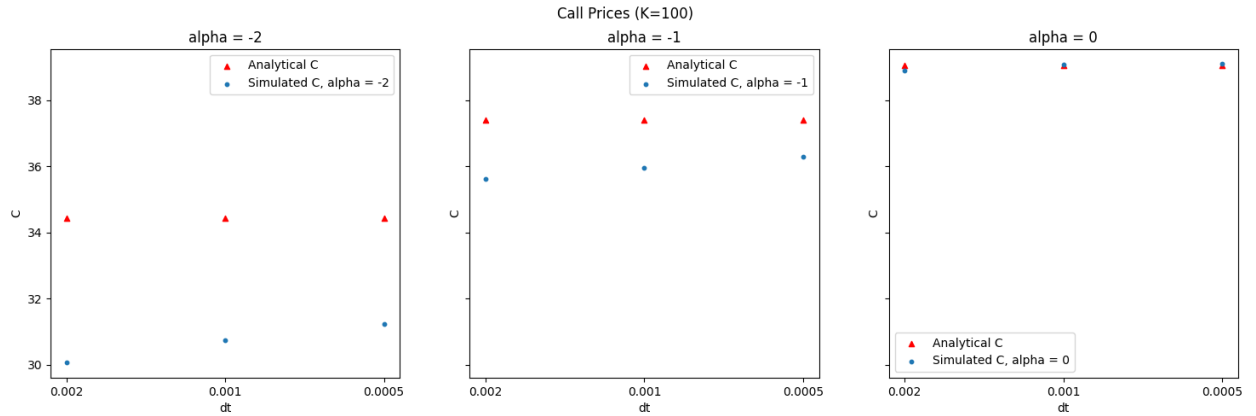


Figure 3: Evaluation of simulated absorption ratio against analytical absorption ratio. Again, deviations in $\alpha < 1$ cas are addressed in Section 3.3



(a) Absorbtion ratio as dt is decreased



(b) Simulated C price as dt is decreased

Figure 4: An analysis of discretization error for $K = 100$ and $\alpha < 0$

4 Conclusions and Future Work

As an exploration of the CEV process, there is not much conclusion to be drawn. However, I found many parts interesting. It was surprising that F could be transformed into a well-known Bessel function, such that the resulting transition density function was related to the non-central chi-squared distribution. Additionally, the absorption actually follows a function. This was intriguing to confirm via path simulations. Additionally, it was surprising that the Euler scheme would start failing drastically for certain parameter schemes despite nothing wrong with the values. Significantly smaller discretization increments are required to sample $\alpha < 0$ cases. Additionally, the computational cost of the Euler scheme makes it rather infeasible for actual application in a time-sensitive field such as finance.

Future work could explore the $\alpha > 1$ case, more mathematical derivations, or evaluate Monte Carlo Simulations using the method mentioned in [7]. A particularly interesting exploration would be taking real equity data, back-calculating α , computing expected prices, and comparing them to actual prices.

References

- [1] F. Black and M. Scholes. The pricing of options and corporate liabilities. *Journal of Political Economy*, 81(3):637–654, 1973.
- [2] J. C. Cox. The constant elasticity of variance option pricing model. *The Journal of Portfolio Management*, 23(5):15–17, 1996.
- [3] W. Feller. Two singular diffusion problems. *The Annals of Mathematics*, 54(1):173, 1951.
- [4] H. Geman and Y. F. Shih. Modeling commodity prices under the cev model. *The Journal of Alternative Investments*, 11(3):65–84, 2008.
- [5] Y. Hsu, T. Lin, and C. Lee. Constant elasticity of variance (cev) option pricing model: Integration and detailed derivation. *Mathematics and Computers in Simulation*, 79(1):60–71, 2008.
- [6] J. Hull. *Options, futures, and other derivatives*. Pearson Education Limited, 2022.
- [7] A. Lindsay and D. Brecher. Simulation of the cev process and the local martingale property. *Mathematics and Computers in Simulation*, 82(5):868–878, 2012.
- [8] M. SCHRODER. Computing the constant elasticity of variance option pricing formula. *The Journal of Finance*, 44(1):211–219, 1989.
- [9] J. Yu. On leverage in a stochastic volatility model. *Journal of Econometrics*, 127(2):165–178, 2005.

A Verification of Squared Bessel Process

$$\begin{aligned}
X &= \frac{F^{2(1-\alpha)}}{\sigma^2(1-\alpha)^2}, \quad dX = \delta dt + \sigma\sqrt{X}dW, \quad \delta = \frac{1-2\alpha}{1-\alpha} \\
dF &= \sigma F^\alpha dW = A(x)dt + B(x)dW \\
A(x) &= 0, B(x) = \sigma F^\alpha, X_t = 0, X_{F(x)} = \frac{2F^{1-2\alpha}}{(1-\alpha)\sigma^2}, X_{F(x),F(x)} = \frac{(4\alpha-2)F^{-2\alpha}}{(\alpha-1)\sigma^2k} \\
dX &= (X_t + X_{F(t)}A(t) + \frac{1}{2}X_{F(t),F(t)}B(t)^2)dt + (X_{F(t)}B(t))dW \\
&= (0 + 0 + \frac{1}{2}\frac{(4\alpha-2)F^{-2\alpha}}{(\alpha-1)\sigma^2}(\sigma F^\alpha)^2)dt + (\frac{2F^{1-2\alpha}}{(1-\alpha)\sigma^2}\sigma F^\alpha)dW \\
&= \frac{(1-2\alpha)}{(1-\alpha)}dt + 2\frac{F^{1-\alpha}}{\sigma(1-\alpha)}dW \\
&= \delta dt + 2\sqrt{X}dW \quad \delta = \frac{(1-2\alpha)}{(1-\alpha)}
\end{aligned} \tag{14}$$

B Results

Table 1: Simulated Call and Put values for $K = 90$

| α | Simulated Calls | Analytical Calls | Simulated Puts | Analytical Puts |
|-------------|------------------|------------------|------------------|-----------------|
| -2.0 | 36.18731±0.03790 | 40.78008 | 39.01907±0.04450 | 30.78008 |
| -1.0 | 41.51010±0.04638 | 43.22324 | 36.54361±0.04374 | 33.22324 |
| 0.0 | 43.96978±0.06202 | 43.98810 | 34.13850±0.04090 | 33.98810 |
| 0.1 | 43.86517±0.06429 | 43.81491 | 33.86517±0.04021 | 33.81491 |
| 0.2 | 43.52320±0.06678 | 43.58715 | 33.54140±0.03935 | 33.58715 |
| 0.3 | 43.39890±0.06984 | 43.31587 | 33.30209±0.03837 | 33.31587 |
| 0.4 | 43.01630±0.07303 | 43.02013 | 32.97611±0.03721 | 33.02013 |
| 0.5 | 42.86400±0.07700 | 42.72311 | 32.67832±0.03588 | 32.72311 |
| 0.6 | 42.45335±0.08145 | 42.44314 | 32.43711±0.03451 | 32.44314 |
| 0.7 | 42.23271±0.08694 | 42.18755 | 32.17374±0.03313 | 32.18755 |
| 0.8 | 41.97058±0.09372 | 41.95654 | 32.01302±0.03183 | 31.95654 |
| 0.9 | 41.46066±0.10218 | 41.74881 | 31.75865±0.03059 | 31.74881 |

Table 2: Simulated Call and Put values for $K = 100$

| α | Simulated Calls | Analytical Calls | Simulated Puts | Analytical Puts |
|----------|------------------------|------------------|------------------------|-----------------|
| -2.0 | 30.68502 \pm 0.03374 | 34.42928 | 43.53105 \pm 0.04934 | 34.42928 |
| -1.0 | 35.95739 \pm 0.04249 | 37.38750 | 41.05997 \pm 0.04841 | 37.38750 |
| 0.0 | 38.92345 \pm 0.05834 | 39.04516 | 39.21799 \pm 0.04509 | 39.04516 |
| 0.1 | 38.95621 \pm 0.06084 | 39.00887 | 39.09999 \pm 0.04434 | 39.00887 |
| 0.2 | 38.87104 \pm 0.06345 | 38.93070 | 38.98962 \pm 0.04346 | 38.93070 |
| 0.3 | 38.95016 \pm 0.06670 | 38.82097 | 38.76909 \pm 0.04238 | 38.82097 |
| 0.4 | 38.85327 \pm 0.07012 | 38.69619 | 38.66758 \pm 0.04116 | 38.69619 |
| 0.5 | 38.58408 \pm 0.07369 | 38.57528 | 38.57982 \pm 0.03979 | 38.57528 |
| 0.6 | 38.54010 \pm 0.07852 | 38.47236 | 38.46275 \pm 0.03836 | 38.47236 |
| 0.7 | 38.31322 \pm 0.08392 | 38.39279 | 38.37608 \pm 0.03694 | 38.39279 |
| 0.8 | 38.21156 \pm 0.09111 | 38.33676 | 38.33880 \pm 0.03558 | 38.33676 |
| 0.9 | 38.30854 \pm 0.10052 | 38.30351 | 38.25522 \pm 0.03429 | 38.30351 |

Table 3: Simulated Call and Put values for $K = 110$

| α | Simulated Calls | Analytical Calls | Simulated Puts | Analytical Puts |
|----------|------------------------|------------------|------------------------|-----------------|
| -2.0 | 25.35551 \pm 0.02964 | 28.28014 | 48.16271 \pm 0.05409 | 38.28014 |
| -1.0 | 30.73917 \pm 0.03872 | 31.81087 | 45.69526 \pm 0.05293 | 41.81087 |
| 0.0 | 34.41975 \pm 0.05496 | 34.44670 | 44.60033 \pm 0.04917 | 44.44670 |
| 0.1 | 34.49657 \pm 0.05737 | 34.55387 | 44.63636 \pm 0.04836 | 44.55387 |
| 0.2 | 34.70268 \pm 0.06019 | 34.63001 | 44.65760 \pm 0.04742 | 44.63001 |
| 0.3 | 34.60384 \pm 0.06297 | 34.68438 | 44.72490 \pm 0.04627 | 44.68438 |
| 0.4 | 34.69962 \pm 0.06651 | 34.73094 | 44.66912 \pm 0.04499 | 44.73094 |
| 0.5 | 34.70750 \pm 0.07037 | 34.78498 | 44.74605 \pm 0.04357 | 44.78498 |
| 0.6 | 34.77222 \pm 0.07520 | 34.85746 | 44.78326 \pm 0.04209 | 44.85746 |
| 0.7 | 35.09838 \pm 0.08136 | 34.95247 | 44.87004 \pm 0.04061 | 44.95247 |
| 0.8 | 35.05481 \pm 0.08821 | 35.07041 | 45.05617 \pm 0.03923 | 45.07041 |
| 0.9 | 35.15077 \pm 0.09764 | 35.21113 | 45.22257 \pm 0.03786 | 45.21113 |